Targeted Detection of Cyclooxygenase-1 in Ovarian Cancer

Paola Malerba,[†,‡] Brenda C. Crews,[†] Kebreab Ghebreselasie,[†] Cristina K. Daniel,[†] Elma Jashim,[†] Ansari M. Aleem,[†] Redoan A. Salam,[†,∥] Lawrence J. Marnett,[†] and Md. Jashim Uddin*[,†]

[†]A. B. Hancock, Jr. Memorial Laboratory for Cancer Research, Departments of Biochemistry, Chemistry, and Pharmacology, Vanderbilt Institute of Chemical Biology, Vanderbilt-Ingram Cancer Center, Vanderbilt University School of Medicine, Nashville, Tennessee 37232 United States

[‡]Department of Pharmacy and Pharmaceutical Sciences, University of Bari "A. Moro", Via Orabona 4, 70125 Bari, Italy

[∥]Department of Biology, Washington University in St. Louis, St. Louis, Missouri 63130 United States

Ⓢ Supporting Information

ABSTRACT: Overexpression of cyclooxygenase-1 (COX-1) is associated with the initiation and progression of ovarian cancer, and targeted imaging of COX-1 is a promising strategy for early detection of this disease. We report the discovery of N-[(5-carboxy-X-rhodaminyl)but-4-yl]-3-(1-(4-methoxyphenyl)-5-(p-tolyl)-1H-pyrazol-3-yl)propenamide (CMP) as the first COX-1-targeted optical agent for imaging of ovarian cancer. CMP exhibits light emission at 604 nm (λ_{max}), thereby minimizing tissue autofluorescence interference. In both purified enzyme and COX-1-expressing human ovarian adenocarcinoma (OVCAR-3) cells, CMP inhibits COX-1 at low nanomolar potencies (IC_{50} = 94 and 44 nM, respectively). CMP's selective binding to COX-1 in OVCAR-3 cells was visualized microscopically as intense intracellular fluorescence. In vivo optical imaging of xenografts in athymic nude mice revealed COX-1-dependent accumulation of CMP in COX-1-expressing mouse ovarian surface epithelial carcinoma (ID8-NGL) and OVCAR-3 cells. These results establish proof-of-principle for the feasibility of targeting COX-1 in the development of new imaging and therapeutic strategies for ovarian cancer.

KEYWORDS: Optical imaging, cyclooxygenase-1, ovarian cancer, COX-1-selective inhibitor, CMP probe
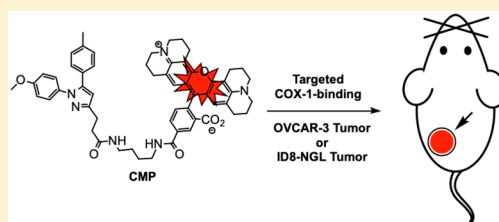
The cyclooxygenase enzymes (COX-1 and COX-2) catalyze the initial, rate-limiting step in the conversion of arachidonic acid to prostaglandins (PGs) and thromboxane. Expression patterns of the two enzyme isoforms support the hypothesis that COX-1 plays a predominantly homeostatic role, whereas COX-2 is a key modulator of inflammation, cellular proliferation, and tumorigenesis.[1,2] In fact, COX-2 overexpression is a well-documented phenomenon in many forms of cancer.[3,4] An exception to these generalities, however, is seen in the case of ovarian cancer, in which COX-1 is frequently overexpressed and believed to contribute significantly to disease initiation and progression.[5] For example, Li and co-workers reported COX-1 expression in seven out of nine ovarian carcinoma cell lines, whereas COX-2 expression was not detectable.[6] In addition, elevated COX-1 but not COX-2 expression was detected in genetically engineered murine ovarian cancer cell lines that lack p53 and overexpress either myc and K-ras or myc and akt. Tumors derived by orthotopic implantation of these cell lines in nude mice also expressed high levels of COX-1, and growth of one of them in vivo was suppressed by the COX-1-selective inhibitor SC-560, but not the COX-2-selective inhibitor celecoxib.[7] Studies suggest that PGs derived from COX-1-dependent oxygenation of arachidonic acid play an important role in multiple events associated with growth, survival, and metastasis of ovarian cancer.[8] Motz et al. reported that COX-1-derived PGE2

diffuses from ovarian cancers and cooperates with vascular endothelial growth factor to induce release of Fas ligand from vascular endothelial cells. Fas ligand acts on CD8^{+} T cells to induce apoptosis, thereby preventing their cytotoxic action on ovarian cancer cells. Thus, the combination of a vascular endothelial growth factor receptor kinase inhibitor with aspirin (a nonselective COX inhibitor) dramatically inhibited the growth of ovarian cancers in vivo.[9] Recently, a large consortium that pooled analyses of 12 studies demonstrated that daily low-dose aspirin confers a 20 to 34% reduction in the risk of developing ovarian cancer.[10] Furthermore, large observational studies in patients show that regular use of aspirin, even at low doses, reduces the long-term risk of distant metastases, particularly in the case of adenocarcinomas.[11] These results support the functional significance of COX-1 in ovarian cancer and the potential value of COX-1-targeted imaging and therapeutic agents in the management of this neoplastic disease.

Clinical diagnosis of ovarian cancer in its early stages is a major unmet medical need. Existing strategies for diagnosis of
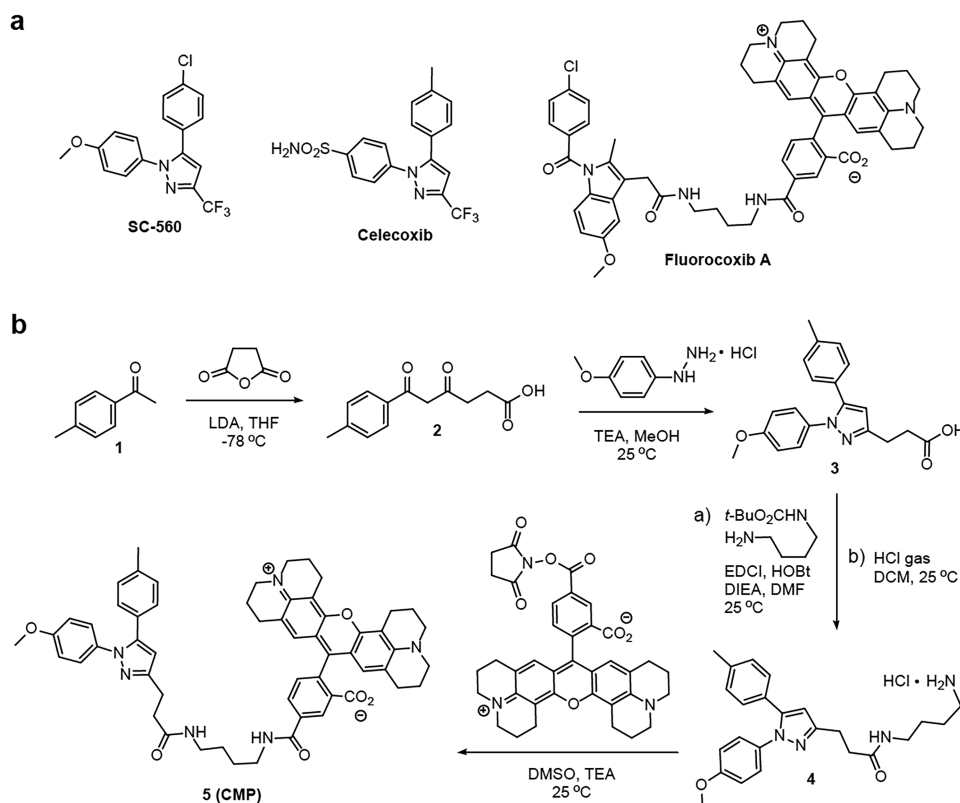
Figure 1. (a) Structures of SC-560, celecoxib, and fluorocoxib A, and (b) chemical synthesis of CMP.

ovarian cancer include ultrasound, computed tomography, magnetic resonance imaging, position emission tomography (PET), and laparoscopy. Among these methods, only PET employs contrast agents, such as [^{18}F]fluorodeoxyglucose ([^{18}F]FDG), for visualization. In fact, [^{18}F]FDG-PET has been evaluated for the diagnosis of ovarian cancer in a number of clinical studies,[12] but it has not demonstrated adequate specificity or sensitivity in these settings.[13,14] Other imaging agents that have been developed so far have shown some promise in animal models of ovarian cancer, but none has progressed into clinical trials. Our laboratory has made major contributions to the development of targeted imaging[15−19] and therapeutic agents[20,21] for cancer. We discovered the first COX-2-targeted optical imaging agent (fluorocoxib A)[15] and cancer chemotherapeutic agent (chemocoxib A),[20] and we have also discovered COX-2-targeted PET and single-photon emission computed tomography agents for imaging of cancer and inflammation.[22,23] Herein, we report the first COX-1-targeted optical imaging agent N-[(5-carboxy-X-rhodaminyl)-but-4-yl]-3-(1-(4-methoxyphenyl)-5-(p-tolyl)-1H-pyrazol-3-yl)propenamide (CMP) and demonstrate its feasibility in the COX-1-dependent in vivo visualization of human ovarian tumor xenografts.

The discovery of the COX-2-targeted imaging agent fluorocoxib A (Figure 1a) was accomplished through the conjugation of a fluorescent moiety to the carboxyl group of the nonselective COX inhibitor indomethacin via a hydrocarbon tether. The resulting compound exhibited COX-2-selective inhibitory activity, and we found that we could, in fact, generate a wide variety of fluorescent inhibitors in this fashion.[19] The X-ray crystal structures of fluorescent indomethacin−dansyl conjugates in complex with COX-2 revealed that the indomethacin moiety adopts a binding pose

in the enzyme's active site very similar to that of the parent compound and that the tether extends through a constriction at the opening of the active site, placing the dansyl moiety in the lobby, an alcove within the protein's membrane binding domain.[24] The relatively spacious lobby allows it to accommodate conjugates as large as 5-carboxy-X-rhodamine as is found in fluorocoxib A. We hypothesize that we could apply the same general strategy to develop a COX-1-targeted optical imaging agent, starting with the COX-1-selective inhibitor SC-560 as a scaffold. An X-ray crystal structure of mefozolac, a COX-1-selective diarylheterocycle similar to SC-560, in complex with COX-1 revealed a binding orientation that placed the inhibitor's five-membered heterocyclic ring close to the constriction, suggesting that attaching the tether to this ring would most likely lead to success.[25]

To test this hypothesis, we synthesized CMP using a multistep reaction scheme (Figure 1b; full compound names are provided in the Supporting Information). Briefly, the Claisen condensation of compound **1** with succinic anhydride in the presence of lithium diisopropylamide proceeded smoothly to afford compound **2**. Condensation of **2** with (4-methoxyphenyl)hydrazine hydrochloride afforded compound **3**. After the 1,5-regioisomer was separated from the minor 1,3-regioisomer by flash chromatography, **3** was then reacted with tert-butyl (4-aminobutyl)carbamate in the presence of ethyl-1-[3-(dimethylamino)propyl]-3-ethylcarbodiamide to give a carbamate intermediate, which was then treated with hydrogen chloride gas to afford compound **4**. 5-Carboxy-X-rhodamine-acid was activated using N,N,N′,N′-tetramethyl-O-(N-succinimidyl)uronium tetrafluoroborate in the presence of triethylamine and coupled with **4** to yield the target fluorescent conjugate CMP (compound **5**). CMP emitted bright red-shifted fluorescence with excitation and emission maxima of λ_{ex}
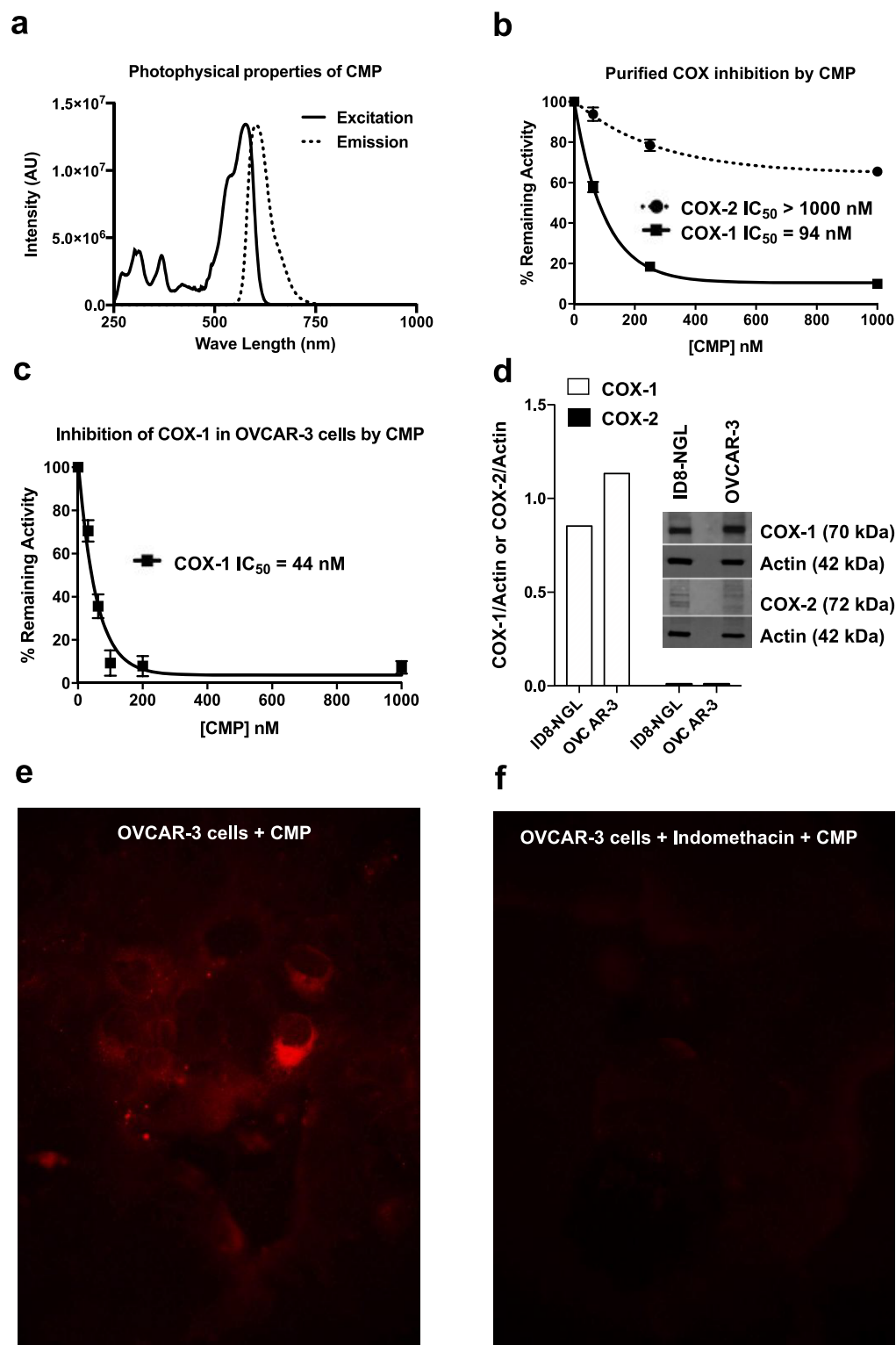
Figure 2. (a) Photophysical properties of CMP; (b) purified COX-1 and COX-2 inhibition profiles of CMP; (c) cellular COX-1 inhibition profile of CMP in OVCAR-3 cells; (d) immunoblot showing the expression of COX-1 and COX-2 in the ID8-NGL and OVCAR-3 cell lines; (e) optical imaging of COX-1 in OVCAR-3 cells; (f) imaging of COX-1 in OVCAR-3 cells pretreated with indomethacin (5 μM).

= 580 nm and λ_{em} = 606 nm, respectively, and a quantum yield of 0.95 at 604 nm (Figure 2a). The compound's molar extinction coefficient was 35/mM/cm at 580 nm. These optical properties are desirable for an in vivo optical imaging agent, as they help to minimize the problem of autofluorescence interference from live tissues.

The ability of CMP to inhibit purified COX-1 or COX-2 was evaluated in a thin layer chromatography assay using [1-^{14}C]arachidonic acid as substrate.[15] Briefly, purified ovine COX-1 or murine COX-2 was preincubated with vehicle or CMP at various concentrations for 20 min followed by substrate addition and incubation for an additional 30 s.

Termination solution was added, and the products were extracted, spotted, developed, and scanned for $[1\text{-}^{14}C]$-arachidonic acid remaining. CMP displayed selective and potent COX-1 inhibitory activity (COX-1 IC_{50} = 94 nM; COX-2 IC_{50} > 1000 nM) (Figure 2b). Inhibition of COX-1 in intact cells by CMP was also evaluated using a previously described method.[15] COX-1-expressing OVCAR-3 cells were treated with vehicle or CMP at different concentrations for 30 min followed by addition of $[1\text{-}^{14}C]$arachidonic acid and incubation for 30 min more. Aliquots of the culture medium were transferred to termination solution, extracted, spotted, developed, and scanned for $[1\text{-}^{14}C]$arachidonic acid remaining. The IC_{50} value for inhibition of human COX-1 by CMP in OVCAR 3 cells was 44 nM (Figure 2c).

Using commercially available specific antibodies, we tested the levels of COX-1 and COX-2 in human OVCAR-3 ovarian cancer cells and ID8-NGL murine ovarian surface epithelial cancer cell lines by immmunoblot analysis. We used purified COX-1 and COX-2 as standards and β-actin as a loading control. We detected high levels of COX-1 expression in OVCAR3 and ID8-NGL cells as compared to minimal COX-2 expressions in these cell lines (Figure 2d). ImageJ software version 1.52K (National Institutes of Health, USA) was used to analyze the intensity of obtained bands. The immmunoblot data suggest these cell lines will be suitable for evaluating and validating the feasibility of CMP in vitro and in vivo.

We evaluated the ability of CMP to fluorescently label COX-1 in OVCAR-3 cells in culture. Following pretreatment of the cells with vehicle or indomethacin for 30 min, the cells were incubated with CMP for an additional 30 min, washed briefly, and then cultured in serum-containing medium for 45 min. The purpose of indomethacin pretreatment was to block the active site of COX-1, thereby preventing uptake and retention of CMP. Optical imaging under a fluorescence microscope revealed that vehicle-pretreated cells were reproducibly labeled by CMP (Figure 2e), whereas minimal fluorescence was observed in indomethacin-pretreated cells (Figure 2f). The results suggest that CMP's fluorescence labeling in vehicle-treated cells was COX-1-dependent. Notably, the dispersed cytoplasmic fluorescence signals denote a diffuse expression of COX-1 in these cells.

We validated CMP as a COX-1-targeted optical imaging agent in two different mouse tumor models of ovarian cancer using a protocol approved by the Vanderbilt Institutional Animal Care and Use Committee. First, we evaluated the ability of CMP to detect COX-1 in xenografts derived from OVACR-3 cells. In each female athymic nude mouse, OVCAR-3 cells were implanted subcutaneously on the left hind flanks. The xenografts were allowed to grow to approximately 750–1000 mm^3 to ensure that a vascular bed was established. Mice were then administered CMP intraperitoneally (i.p., 1 mg/kg in dimethyl sulfoxide (DMSO)), and at 15 min, 30 min, 1 h, 2 h, 3 h, and 4 h postinjection, they were lightly anesthetized and placed in an IVIS imaging system. No detectable level of CMP uptake was observed at any time points before 2 h postinjection. However, at 3 to 4 h postinjection, we detected reproducible, high tumor fluorescence as compared to leg muscle signals (Figure 3a). To further check the biodistribution, after in vivo imaging, we collected tumor, muscle, kidney, and liver from OVCAR-3 tumor-bearing animals and imaged them ex vivo (Figure 3b). The ex vivo quantification showed high CMP accumulation in the OVCAR-3 tumors (Figure 3c) compared to the other tissues ($n = 4$, $p < 0.004$).
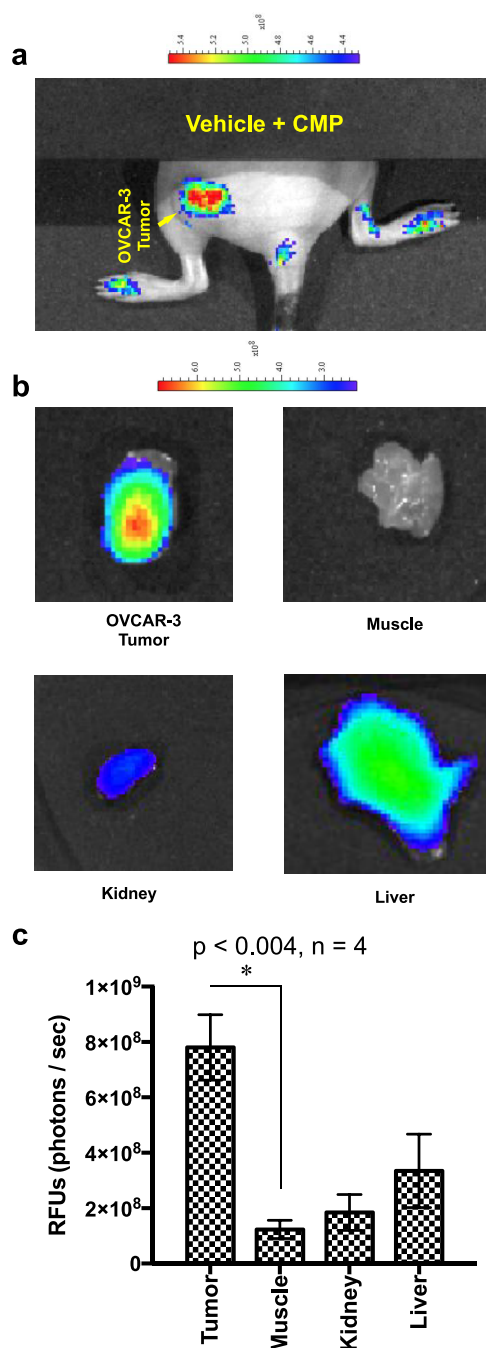

Figure 3. (a) In vivo imaging of COX-1 in an OVACR-3 tumor by CMP; (b) ex vivo imaging of an OVACR-3 tumor compared with leg muscle, kidney, and liver; (c) region of interest measurements of light emission from OVACR-3 tumor, leg muscle, kidney, and liver (CMP, t = 3.5 h) (RFU, relative fluorescence units).

We evaluated the utility of CMP in COX-1-targeted imaging of ovarian tumors derived from ID8-NGL cells implanted into the left hind flanks of nude mice ($n = 6$ animals) using a procedure similar to that described above. For imaging, we administered CMP i.p. (2 mg/kg in DMSO) to mice bearing full grown tumors (750 to 1000 mm^3). The animals were imaged under light anesthesia at 3 to 4 h postinjection of CMP. The ID8-NGL tumors exhibited strong fluorescence signals (Figure 4a and Supplemental Figure S1). After in vivo imaging, we euthanized the animals and collected the ID8-
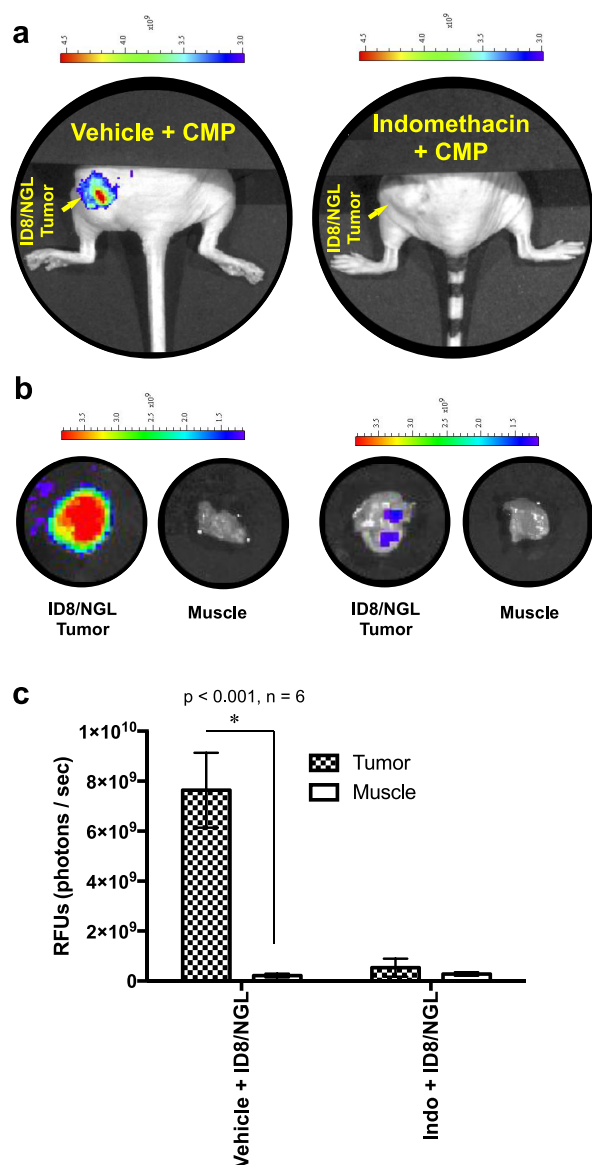
Figure 4. (a) In vivo optical imaging of COX-1 in ID8-NGL tumor (left mouse) and indomethacin-pretreated ID8-NGL tumor (right mouse); (b) ex vivo imaging of ID8-NGL (left mouse) and indomethacin-pretreated ID8-NGL (right mouse) tumors compared with leg muscle; (c) region of interest measurements of light emission from ID8-NGL tumor and indomethacin-pretreated ID8-NGL tumor at 3.5 h postinjection of CMP (RFU, relative fluorescence units).

NGL tumors and surrounding muscle for *ex vivo* imaging (Figure 4b). Based on the measurements of light emission, the uptake of CMP in the ID8-NGL tumors was ∼8-fold higher than that in the muscle (Figure 4c). We elucidated the mechanism of the COX-1-targeted delivery and binding of CMP in ID8-NGL tumor allografts by administering a high dose (10 mg/kg in DMSO) of indomethacin i.p. to tumor-bearing mice 1 h prior to CMP (i.p., 2 mg/kg in DMSO). At 3 to 4 h post-CMP injection, optical imagining revealed extremely low levels of fluorescence in the tumors, suggesting effective COX-1 blockade by indomethacin (Figure 4a−c). These findings support the hypothesis that uptake and retention of CMP in the tumor was COX-1-dependent.

In conclusion, we describe the discovery of CMP, a COX-1-targeted optical imaging agent. CMP exhibits light emission at

604 nm and inhibits COX-1 at low nanomolar potencies in both purified enzyme preparations and ovarian cancer cell lines. *In vivo* optical imaging shows selective uptake of CMP in COX-1-overexpressing mouse tumors derived from human ovarian cancer (OVCAR-3) cells and mouse ovarian surface epithelial carcinoma (ID8-NGL) cells. Uptake of CMP is COX-1-dependent as confirmed by failure of CMP uptake in indomethacin-pretreated mouse tumors derived from COX-1-overexpressing ID8-NGL cells. These data provide support for the feasibility of targeting COX-1 in pathological tissues. CMP represents the first COX-1-targeted *in vivo* optical imaging agent validated for visualization of tissues, such as the neoplastic tissues in the ovary, overexpressing the enzyme.

■ ASSOCIATED CONTENT

Ⓢ Supporting Information

The Supporting Information is available free of charge on the ACS Publications website at DOI: 10.1021/acsmedchem-lett.9b00280.

Chemical synthesis and spectroscopic characterization of compounds **2** through **5**, methods for animal experiments, and Figure S1 (PDF)

■ AUTHOR INFORMATION

Corresponding Author
*Phone: 615-484-8674. E-mail: jashim.uddin@vanderbilt.edu.

ORCID Ⓞ
Lawrence J. Marnett: 0000-0002-7834-6285
Md. Jashim Uddin: 0000-0003-0020-4866

Author Contributions
P.M. synthesized and characterized all the raw materials and the final compound CMP; B.C.C. performed animal and cell imaging experiments; K.G. biochemically evaluated the compounds; C.K.D. carried out cell-based testing of compounds; E.J. purified a sample of CMP for testing and deposited CMP for institutional registration; A.M.A. quantified protein expression by immunoblot analysis, R.A.S. synthesized a batch of CMP, L.J.M. provided laboratory space and financial support, and M.J.U. conceived the idea, designed the experiments, interpreted the data, wrote the manuscript, and supervised the overall conduct of the research program. All authors have given approval to the final version of the manuscript.

of the A. B. Hancock, Jr. Memorial Laboratory for Cancer Research for critical reading and editing of the manuscript.

REFERENCES

(1) Rouzer, C. A.; Marnett, L. J. Non-redundant functions of cyclooxygenases: oxygenation of endocannabinoids. *J. Biol. Chem.* **2008**, *283*, 8065−8069.

(2) Smith, W. L.; Garavito, R. M.; DeWitt, D. L. Prostaglandin endoperoxide H synthases (cyclooxygenases)-1 and −2. *J. Biol. Chem.* **1996**, *271*, 33157−33160.

(3) Harris, R. E. Cyclooxygenase-2 (cox-2) and the inflammogenesis of cancer. *Subcell. Biochem.* **2007**, *42*, 93−126.

(4) Hashemi Goradel, N.; Najafi, M.; Salehi, E.; Farhood, B.; Mortezaee, K. Cyclooxygenase-2 in cancer: A review. *J. Cell. Physiol.* **2019**, *234*, 5683−5699.

(5) Wilson, A. J.; Fadare, O.; Beeghly-Fadiel, A.; Son, D. S.; Liu, Q.; Zhao, S.; Saskowski, J.; Uddin, M. J.; Daniel, C.; Crews, B.; Lehmann, B. D.; Pietenpol, J. A.; Crispens, M. A.; Marnett, L. J.; Khabele, D. Aberrant over-expression of COX-1 intersects multiple pro-tumorigenic pathways in high-grade serous ovarian cancer. *Oncotarget* **2015**, *6*, 21353−21368.

(6) Li, S.; Miner, K.; Fannin, R.; Carl Barrett, J.; Davis, B. J. Cyclooxygenase-1 and 2 in normal and malignant human ovarian epithelium. *Gynecol. Oncol.* **2004**, *92*, 622−627.

(7) Daikoku, T.; Wang, D.; Tranguch, S.; Morrow, J. D.; Orsulic, S.; DuBois, R. N.; Dey, S. K. Cyclooxygenase-1 is a potential target for prevention and treatment of ovarian epithelial cancer. *Cancer Res.* **2005**, *65*, 3735−3744.

(8) Gupta, R. A.; Tejada, L. V.; Tong, B. J.; Das, S. K.; Morrow, J. D.; Dey, S. K.; DuBois, R. N. Cyclooxygenase-1 is overexpressed and promotes angiogenic growth factor production in ovarian cancer. *Cancer Res.* **2003**, *63*, 906−911.

(9) Motz, G. T.; Santoro, S. P.; Wang, L. P.; Garrabrant, T.; Lastra, R. R.; Hagemann, I. S.; Lal, P.; Feldman, M. D.; Benencia, F.; Coukos, G. Tumor endothelium FasL establishes a selective immune barrier promoting tolerance in tumors. *Nat. Med.* **2014**, *20*, 607−615.

(10) Trabert, B.; Ness, R. B.; Lo-Ciganic, W. H.; Murphy, M. A.; Goode, E. L.; Poole, E. M.; Brinton, L. A.; Webb, P. M.; Nagle, C. M.; Jordan, S. J.; Risch, H. A.; Rossing, M. A.; Doherty, J. A.; Goodman, M. T.; Lurie, G.; Kjaer, S. K.; Hogdall, E.; Jensen, A.; Cramer, D. W.; Terry, K. L.; Vitonis, A.; Bandera, E. V.; Olson, S.; King, M. G.; Chandran, U.; Anton-Culver, H.; Ziogas, A.; Menon, U.; Gayther, S. A.; Ramus, S. J.; Gentry-Maharaj, A.; Wu, A. H.; Pearce, C. L.; Pike, M. C.; Berchuck, A.; Schildkraut, J. M.; Wentzensen, N. Aspirin, nonaspirin nonsteroidal anti-inflammatory drug, and acetaminophen use and risk of invasive epithelial ovarian cancer: a pooled analysis in the Ovarian Cancer Association Consortium. *J. Natl. Cancer Inst.* **2014**, *106*, djt431.

(11) Rothwell, P. M.; Wilson, M.; Price, J. F.; Belch, J. F.; Meade, T. W.; Mehta, Z. Effect of daily aspirin on risk of cancer metastasis: a study of incident cancers during randomised controlled trials. *Lancet* **2012**, *379*, 1591−1601.

(12) Rusu, D.; Carlier, T.; Colombie, M.; Goulon, D.; Fleury, V.; Rousseau, N.; Berton-Rigaud, D.; Jaffre, I.; Kraeber-Bodere, F.; Campion, L.; Rousseau, C. Clinical and Survival Impact of FDG PET in Patients with Suspicion of Recurrent Ovarian Cancer: A 6-Year Follow-Up. *Front. Med.* **2015**, *2*, 46.

(13) Lee, S. I.; Catalano, O. A.; Dehdashti, F. Evaluation of gynecologic cancer with MR imaging, ^{18}F-FDG PET/CT, and PET/MR imaging. *J. Nucl. Med.* **2015**, *56*, 436−43.

(14) Tawakol, A.; Abdelhafez, Y. G.; Osama, A.; Hamada, E.; El Refaei, S. Diagnostic performance of ^{18}F-FDG PET/contrast-enhanced CT versus contrast-enhanced CT alone for post-treatment detection of ovarian malignancy. *Nucl. Med. Commun.* **2016**, *37*, 453−460.

(15) Uddin, M. J.; Crews, B. C.; Blobaum, A. L.; Kingsley, P. J.; Gorden, D. L.; McIntyre, J. O.; Matrisian, L. M.; Subbaramaiah, K.; Dannenberg, A. J.; Piston, D. W.; Marnett, L. J. Selective visualization of cyclooxygenase-2 in inflammation and cancer by targeted fluorescent imaging agents. *Cancer Res.* **2010**, *70*, 3618−3627.

(16) Uddin, M. J.; Werfel, T. A.; Crews, B. C.; Gupta, M. K.; Kavanaugh, T. E.; Kingsley, P. J.; Boyd, K.; Marnett, L. J.; Duvall, C. L. Fluorocoxib A loaded nanoparticles enable targeted visualization of cyclooxygenase-2 in inflammation and cancer. *Biomaterials* **2016**, *92*, 71−80.

(17) Uddin, M. J.; Crews, B. C.; Ghebreselasie, K.; Daniel, C. K.; Kingsley, P. J.; Xu, S.; Marnett, L. J. Targeted imaging of cancer by fluorocoxib C, a near-infrared cyclooxygenase-2 probe. *J. Biomed. Opt.* **2015**, *20*, 50502.

(18) Uddin, M. J.; Crews, B. C.; Huda, I.; Ghebreselasie, K.; Daniel, C. K.; Marnett, L. J. Trifluoromethyl fluorocoxib a detects cyclooxygenase-2 expression in inflammatory tissues and human tumor xenografts. *ACS Med. Chem. Lett.* **2014**, *5*, 446−450.

(19) Uddin, M. J.; Crews, B. C.; Ghebreselasie, K.; Marnett, L. J. Design, synthesis, and structure-activity relationship studies of fluorescent inhibitors of cyclooxygenase-2 as targeted optical imaging agents. *Bioconjugate Chem.* **2013**, *24*, 712−723.

(20) Uddin, M. J.; Crews, B. C.; Xu, S.; Ghebreselasie, K.; Daniel, C. K.; Kingsley, P. J.; Banerjee, S.; Marnett, L. J. Antitumor Activity of Cytotoxic Cyclooxygenase-2 Inhibitors. *ACS Chem. Biol.* **2016**, *11*, 3052−3060.

(21) Uddin, M. J.; Smithson, D. C.; Brown, K. M.; Crews, B. C.; Connelly, M.; Zhu, F.; Marnett, L. J.; Guy, R. K. Podophyllotoxin analogues active versus Trypanosoma brucei. *Bioorg. Med. Chem. Lett.* **2010**, *20*, 1787−1791.

(22) Uddin, M. J.; Crews, B. C.; Ghebreselasie, K.; Huda, I.; Kingsley, P. J.; Ansari, M. S.; Tantawy, M. N.; Reese, J.; Marnett, L. J. Fluorinated COX-2 inhibitors as agents in PET imaging of inflammation and cancer. *Cancer Prev. Res.* **2011**, *4*, 1536−1545.

(23) Uddin, M. J.; Crews, B. C.; Ghebreselasie, K.; Tantawy, M. N.; Marnett, L. J. [I]-Celecoxib Analogues as SPECT Tracers of Cyclooxygenase-2 in Inflammation. *ACS Med. Chem. Lett.* **2011**, *2*, 160−164.

(24) Xu, S.; Uddin, M. J.; Banerjee, S.; Duggan, K.; Musee, J.; Kiefer, J. R.; Ghebreselasie, K.; Rouzer, C. A.; Marnett, L. J. Fluorescent indomethacin-dansyl conjugates utilize the membrane-binding domain of cyclooxygenase-2 to block the opening to the active site. *J. Biol. Chem.* **2019**, *294*, 8690−8698.

(25) Cingolani, G.; Panella, A.; Perrone, M. G.; Vitale, P.; Di Mauro, G.; Fortuna, C. G.; Armen, R. S.; Ferorelli, S.; Smith, W. L.; Scilimati, A. Structural basis for selective inhibition of Cyclooxygenase-1 (COX-1) by diarylisoxazoles mofezolac and 3-(5-chlorofuran-2-yl)-5-methyl-4-phenylisoxazole (P6). *Eur. J. Med. Chem.* **2017**, *138*, 661−668.